# Shar pei dermal fibroblasts as a model to investigate hyaluronic acid synthesis and metabolism

G. Zanna*, M.J. Docampo†, D. Fondevila*, A.R.R. Carvalho*, S. Cerrato**, A. Bassols†, L. Ferrer*

*Department of Animal Medicine and Surgery, School of Veterinary Medicine, Universitat Autònoma de Barcelona, 08193 Bellaterra, Barcelona – Spain
**UNIVET, Parque Científico, Universitat Autònoma de Barcelona, 08193 Bellaterra, Barcelona – Spain
†Department of Biochemistry and Molecular Biology, School of Veterinary Medicine, Universitat Autònoma de Barcelona, 08193 Bellaterra, Barcelona – Spain

This work has been accepted as free communication at 24th Annual Congress of the ESVD-ECVD, Florence 2010.

## Abstract

Shar peis are affected by hereditary cutaneous hyaluronosis (HCH), a condition caused by an increased synthesis of hyaluronic acid (HA) by dermal fibroblasts secondary to high HA synthase 2 enzymatic activity. In this study, different microscopic techniques were used to better characterize at cellular level the process of HA synthesis in cultured dermal fibroblasts from shar peis with HCH and from control dogs. By optical microscopy, the actively synthesizing fibroblasts from shar peis adopted a rounded form different from elongated fibroblasts from control animals. By fluorescence microscopy, HA accumulated in diseased fibroblasts, not only extracellularly in a tangled network, but also intracellularly in dense particles at the edge of the cells and in a diffuse pattern. In fibroblasts from control dogs, HA fluorescence was less intense both extracellularly and intracellularly. This fluorescence disappeared after 70 min of digestion of living cells with hyaluronidase, as demonstrated by time-lapse microscopy. By transmission electron microscopy, fibroblasts from shar peis revealed a high number of intracellular dense vesicles corresponding to lysosomes, whereas in control dogs few lysosomes were detected. By scanning electron microscopy, numerous slender cell membrane protrusions, resulting from ongoing HA synthesis, were demonstrated in shar peis, whereas in control dogs these microvilli were less diffusely distributed. In shar peis, these observations were indicative of cells with a highly active HA metabolism. Altogether, these findings further confirmed the key role of dermal fibroblasts and HA in the pathogenesis of HCH, and they demonstrated that shar pei dermal fibroblasts constitute a useful model to investigate HA synthesis and metabolism.

## Introduction

Shar pei dogs are unique among dog breeds. They are known to be affected by hereditary cutaneous mucinosis, a disease manifested as wrinkled and thickened skin, puffy muzzle and/or multiloculated vesicles.[1] These clinical findings are due to an excessive dermal deposition of hylauronic acid (HA), a large unsulfated glycosaminoglycan produced in the skin by dermal fibroblasts.[2,3] As consequence, the term hereditary cutaneous hyaluronosis (HCH) should be used to better describe this entity.

HA is synthesized by three different related hyaluronan synthases (HAS1-HAS2-HAS3) on the inner surface of the plasma membrane to be then extruded out of the cell into the extracellular

space.[4-8] When retained at the cell surface, it can form a pericellular matrix or coat, a micrometer-thick space between the plasma membrane and the extracellular matrix that can be visualized using a suspension of fixed erythrocytes. Intermingled in this transition zone, there are also ectodomains of integral membrane glycoproteins and proteoglycans.[9,10] Many cell types normally without a visible pericellular space, can exhibit one by transfection of HAS[11,12] or after stimulation by epidermal growth factors that activate HAS2.[13] It means that its diameter correlates with the levels of HA synthesis and that its structural integrity is sensitive to inhibitors of HA synthases.[14-16] This coat acts as a highly hydrated environment that protects cells, regulates their spacing during developmental processes, facilitates their migration, and when its production is rapid, cell mitotic detachment and rounding of cells may be promoted.[9] Recent studies using live cell staining have demonstrated that inherent features of HA coats are slender membrane protrusions that largely result from ongoing HA synthesis and that act as a scaffold for the same coat.[17] Scanning electron microscopy of smooth muscle cells revealed these strands as extremely thin structures periodically decorated by large granules corresponding to proteoglycans.[18]

In addition to its role in the extracellular matrix, HA is also present intracellularly as a tangled flocculent network.[19-21] This increased cytoplasmic distribution may result from the uptake of the extracellular HA in cells that have been stimulated to proliferate or it is possible that a synthase localized on an intracellular membrane could be oriented to secrete HA in the cytoplasm.[19]

Despite this background, there are no reports regarding shar peis that describe how the increased HA synthesis that has been shown to occur in consequence of the increased HA synthase-2 mRNA transcription by dermal fibroblasts,[22] could regulate cellular morphology.

Therefore, the first aim of this study was to detect the pericellular matrix in cultured dermal fibroblasts from both shar pei and control dogs using a particle exclusion assay. Secondly, we sought to localize HA extracellularly and intracellularly using confocal scanning laser microscopy technique and, in order to provide a visual evidence of HA digestion after hyaluronidase treatment, we analyzed live cells by time lapse microscopy. Finally, transmission electron microscopy and scanning electron microscopy were used in order to better interpret the interactions that fibroblasts could establish with the surrounding extracellular environment.

## Materials and methods

### *Study population*

Fourteen shar pei dogs from three Spanish shar pei breeders, ranging in age from 2 to 3.5 years, 8 of them females and 6 males, and 5 healthy dogs from other breeds (3 Labradors, one German Shepherd and one mixed breed), all of them females, ranging in age from 2 to 3 years and used as controls, were involved in this study. All shar peis were evaluated at the Veterinary Teaching Hospital of the Universitat Autònoma of Barcelona and considered to be affected by hereditary cutaneous hyaluronosis manifested as thickening, non-pitting puffy skin and wrinkling on the forehead, withers and extremities. All dogs were considered clinically healthy on the basis of normal results of clinical examination, blood and urine analysis. In the shar peis, skin biopsies were taken from the dorsal line using 6 to 8-mm punch biopsy under local anaesthesia. Skin samples from control dogs were instead obtained from the ventral region while animals underwent ovariohysterectomies. Prior to the initiation of the present study, procedures were approved by the

breeders of shar pei dogs, owners of the control dogs and by the Ethical Committee of the Universitat Autònoma of Barcelona.

### *Fibroblast cultures*

Skin samples were washed with phosphate-buffered saline (PBS) solution, chopped into 1 $mm^3$ fragments, and incubated for 140 min in 15 ml of medium per gram of tissue consisting of Dulbecco's modified Eagle's medium (DMEM), containing 300 mg/ml bovine albumin (Sigma, St. Louis, MO, USA), 8 mg/ml protease, 12 mg/ml hyaluronidase, 1 mg/ml DNAse (Sigma), 20 mg/ml bacterial collagenase (Gibco, BRL/Life Technologies, Rockville, MD, USA) and supplemented with 100 IU/ml penicillin and 100 µg/ml streptomycin.

After digestion, cells were washed with PBS, resuspended in DMEM supplemented with 10% fetal calf serum, 100 IU/ml penicillin and 100 µg/ml streptomycin, and grown in a humidified atmosphere at 37ºC with 5% $CO_2$. Growth medium was changed twice weekly until cultures reached subconfluent cell density (70-80%). Cells were observed daily under a Nikon Eclipse TS100 inverted microscope and images acquired by a digital camera Nikon D200 at magnification of 40×. Finally, cells (2 x $10^5$/dish) were seeded on glass coverslip cultures dishes in 10% foetal bovine serum (FBS) DMEM and coverslip cultures were used for immunofluorescence staining.

### *Demonstration of pericellular matrix in fibroblast cultures*

This technique was accomplished by means of a particle-exclusion assay as previously described.[23] Canine red blood cells were fixed in 10% formalin, washed, suspended in PBS ($10^8$ cells/ml), introduced into sparse (50% confluence) fibroblast culture of both shar pei and of controls, and allowed to settle for 15 minutes at 37°C with the plate on the microscope stage. Images were viewed under inverted microscope with 20× and 40× objectives and recorded by photomicrographs.

### *Immunofluorescence analysis*

Coverslip cultures were fixed with 3% paraformaldhehyde (Sigma), 60 mM saccharose in 0.1 M phosphate buffer (PB) for 30 minutes. Samples were permeabilized with 0.25% triton X-100 (Sigma) in PBS for 15 minutes and blocked with 1% bovine albumin. To localize HA, cells were stained with 50 µl/ml of biotinylated HA binding protein (bHABP) (Seikagaku, Tokyo, Japan) at a concentration of 1:100 at 37°C for 1 hour. After 3 washes with PBS, 50 µl of Streptavidin Alexa Fluor® 488-conjugate (Molecular Probes, Invitrogen, Eugene, OR, USA) were used as secondary label. Cell nuclei were counterstained with Hoechst 33342 (Molecular Probes, Eugene, OR, USA) and cell membranes labelled with CellMask™ (Invitrogen, Eugene, OR, USA). The coverslips were then mounted with Fluoroprep mounting medium (bioMérieux, Marcy l'Etoile, France) and stored at 4°C in the dark until analysis. Controls for specificity of HA staining included digestion of cells with 2 U/ml of hyaluronidase from *Streptomyces hyalurolyticus* (Sigma) in 50 mM NaAc 150 mM NaCl pH 6 buffer for 1 hour at 37ºC prior permeabilization.

*Confocal scanning laser microscopy*

The micrographs of fibroblast cells were obtained using a spectral confocal Leica TCS SP5 AOBS (Leica Microsystems, Mannheim, Germany) with an objective Plan-Apochromatic 63× (NA 1.4, oil). Alexa 488 was excited at 488 nm (argon laser) and detected between 500 and 535 nm, CellMask$^{TM}$ stain was excited at 633 nm (helium-neon laser) and detected between 656 and 789 nm, and Hoechst 33342 was excited at 405 nm (blue diode) and detected between 410 and 450 nm. Bi-channel images were acquired in an x-y plane at different intervals along the z-axis.

*Time lapse microscopy and live cell imaging*

Cells seeded in 35-mm glass-bottom MatTek dishes (MatTek Corporation, Ashland, USA) were directly coupled to the fluorescent hyaluronan binding complex, obtained after dissolving the biotinylated HA binding protein in 0.5 ml of 0.1 mM NaAc and incubating it for 2 hr with stirring in Alexa Fluor® 488-conjugate. The probe was dissolved in PBS and diluted to 5 µg/ml final for use. Cell nuclei were counterstained with Hoechst 33342 (Molecular Probes) at 10 µg/ml and cell membranes with CellMask$^{TM}$ at 5 µg/ml. The specificity of the staining for HA was controlled by removing HA with 2 U/ml from hyaluronidase. The images (size of 1024 x 512 pixels, with a 2 line average and a pinhole of 300 µm) were kept at 36ºC temperature and 5% CO2 atmosphere, with a TCS-SP2 AOBS spectral confocal microscope (Leica Microsystems Heidelberg GmbH; Mannheim, Germany) using a Plan-Apochromatic 63× objective (NA 1.4, oil).The time-lapse was performed for 10 hours taking 3 horizontal optical sections every 10 minutes.

*Transmission electron microscopy*

Cells were trypsinized, centrifuged and the resulting pellet fixed in 2.5% glutaraldehyde and 2% paraformaldehyde in PB. They were kept in the fixative for 24 h at 4°C, washed with PB and postfixed with 1.0% osmium tetroxide in PB containing 0.8% potassium ferricyanide at 4ºC. Once dehydrated in acetone, cells were infiltrated with Epon resin over 2 days. Blocks were then embebbed with the same resin and polymerised in an oven for 48 h at 60°C. Ultrathin sections were obtained using a Reichert-Jung Ultracut E ultramicrotome (C. Reichert, Vienna, Austria) and mounted on Formvar-coated cooper grids. Finally sections were stained with 2% uranyl acetate in water and lead citrate, and analyzed using a JEM-2011 transmission electron microscope (Jeol LTD, Tokyo, Japan) with an integrated CCD camera system.

*Scanning electron microscopy*

Cells grown on 13-mm coverslips were fixed with 2.5% glutaraldehyde and 2% paraformaldehyde in PB for 2 h at 4ºC. Then they were washed with PB and postfixed with 1% osmium tetroxide in PB buffer containing 0.8% potassium ferricyanide at 4ºC. Finally, samples were further washed with PB and dehydrated through a graded series of ethanol. After critical point drying, cells were photographed on a JSM-3600 scanning electron microscope (Jeol LTD, Tokyo, Japan).

## Results

### *Fibroblast cultures and pericellular matrix*

By using the inverted microscope Nikon Eclipse TS100 at ×40/0.55, subconfluent fibroblast cells from shar peis tended to have a rounded shape (Figure 1A) in contrast with the elongated, flattened morphology observed in control dogs (Figure 1B). By using the particle exclusion assay, fibroblast cells from shar pei showed to exclude fixed erythrocytes from their surface. Indeed, a clear zone was demonstrated between erythrocytes and fibroblast cell membrane (Figure 2A). Fibroblast cells from control dogs did not show this feature. In this latter case the red blood cells settled immediately adjacent to the fibroblast cell surface (Figure 2B).

### *Confocal scanning laser microscopy*

Transmitted light images (also taken with the CSLM, using the 488 nm laser line from the Argon Laser) showed that rounded fibroblasts from shar pei were expanded on their surface by long protrusions (Figure 3A) that disappeared after digestion of the cells with *Streptomyces hyalurolyticus* hyaluronidase (Figure 3B). Elongated cells from controls showed short protrusions projecting out from the cell surface (Figure 3C) that also disappeared after hyaluronidase treatment (Figure 3D). Fluorescein-labelled HA was detected in rounded fibroblasts of shar peis as a tangled flocculent green network diffusely distributed around the cells and also intracellularly (Figure 4A). Fibroblasts labelled with CellMask™ dye, showed broad expanded protrusions extending from the cell membrane (Figure 4B) such as also evidenced in micrographs obtained after merging of images (Figure 4C). The extracellular green fluorescence disappeared after digestion of cells with hyaluronidase (Figure 4D), and a retraction of cell membrane protrusions was observed especially in fibroblasts labelled with CellMask™ cell membrane dye (Figure 4E) such as in micrographs obtained after merging of images (Figure 4F).

In control dogs, elongated fibroblasts appeared weakly stained extracellularly by a green fluorescence. This fluorescence was also weakly intense intracellularly and without formation of dense particles (Figure 5A). Short membrane protrusions were also detected and better evidenced after labelling cells with CellMask™ dye (Figure 5B) and after merging of images (Figure 5C). Green staining disappeared after digestion of cells with hyaluronidase (Figure 5D), and a retraction of the short membrane protrusions was better observed after labelling cells with CellMask™ cell membrane dye (Figure 5E) and after merging of images (Figure 5F).

In the permeabilized cells of shar peis, there was a prominent cytoplasmic fluorescence that appeared both in dense green particles at the borders and in a diffuse pattern throughout the cytoplasm of cells (Figure 6A). Cells were also labelled with CellMask™ cell membrane dye (Figure 6B) and green fluorescence was also observed in micrographs obtained after merging of images (Figure 6C). In fibroblasts from controls, green fluorescence was always diffuse but appeared less intense and without formation of dense peripheral particles (data not shown).

### *Time lapse confocal microscopy*

Hyaluronidase applied on living cells, labelled with biotinylated HA binding protein, with CellMask™ membrane dye and Hoechst 33342 nuclei dye, gradually removed hyaluronan green fluorescence

from fibroblasts from shar peis, until to obtain the total disappearance of fluorescence after 70 minutes from digestion together with a retraction of cell membrane protrusions (Figure 7).

### *Transmission electron microscopy (TEM)*

Rounded fibroblasts from shar peis showed multiple long tortuous and convoluted lamellipodia-like protrusions polarized on a side of the cell and showed to establish connections with neighboring cells. Intracellularly, multiple spherical dense particles, lying just below lamellipodia were observed and considered to be lysosomes (Figure 8A). All these findings were better appreciated at higher magnification (Figure 8B). In fibroblasts from controls, protrusions appeared as few, thin, short structures diffusely distributed at cell surface and also forming connections with other cells. Intracellularly, dense and diffuse particles corresponding to lysosomes were observed in scattered fibroblasts (Figure 8C). All these findings were better appreciated at higher magnification (Figure 8D).

### *Scanning electron microscopy (SEM)*

In shar peis, rounded cells were observed to be covered by individual and multiple slender microvillus-type protrusions (Figure 9A). Dense and globular corpuscles were also observed on the edge of the cell from which the thread-like structures often decorated by dense particles appeared to emerge (Figure 9B). In controls, elongated fibroblasts showed less diffuse filamentous-like structures (Figure 9C), mostly extending from the flattened flanks of the cells and decorated by scattered granules (Figure 9D).

## Discussion

The goal of the present study was to investigate how an increased synthesis of HA by dermal fibroblasts could influence cellular morphology and therefore the adaptive interactions that fibroblasts establish with the surrounding extracellular environment.

The first finding was to observe that fibroblasts from shar peis tended to have a rounded shape and to produce a voluminous pericellular matrix in comparison with the elongated shape and the lack of coat observed in control dogs.

In humans, visual evidence for a dynamic causal relationship between the formation of the cell coat and a subsequent cell detachment and mitotic cell rounding, has been demonstrated and hypothesized to be due to the steric exclusion properties of the same cell coat.[24] To further corroborate this hypothesis, there is a study in time lapse microscopy in conjunction with a particle exclusion assay that provided a visual evidence of how a rapid pericellular matrix formation accompanied the detachment and rounding of cells.[19] Indeed, it was concluded that when the formation of a concentrated HA- dependent pericellular coat on the undersurface of cultured cells is rapid, cells are induced to come off from the substrate to which they adhere because it is like if the same coat provides them a countervailing force.

This conclusion could also relate to the same properties of the coat that, as a highly hydrated

structure with a low content of organic material,[25] functions as a lubricative anti-adhesive means that creates a guidance for cell migration and proliferation.[19] On the contrary, when the coat is produced in small or no amounts, cells appear flattened and highly spread as if they need to create a stable structure on the substrate to which they tightly adhere.[10]

In our study, for want of a treatment with hyaluronidase, we could only hypothesize that the thick exclusion space detected in shar peis could be the direct consequence of the increased, accelerated HA synthesis to which to correlate the rounding of cells. On the contrary, the elongated fibroblast shape, with long, trailing processes and relatively little HA-dependent pericellular matrix detected in controls, was hypothesized to depend on a low HA synthesis.

Transmitted light images showed fibroblasts from shar peis with long expanded protrusions extending at the leading edge of the cells and disappearing after digestion with hyaluronidase. The same protrusions were also detected by confocal scanning laser microscopy as extending filipodia surrounded by a diffuse flocculent green fluorescence corresponding to HA staining. By staining cells with a dye specific for membranes, these protrusions proved to be extensions of the same cellular membrane. In controls, these extensions that also disappeared after hyaluronidase treatment and that were also demonstrated to be membrane-dependent, showed to be shorter and surrounded by a faint green fluorescence.

Microvillus-type cell protrusions represent a distinct cellular compartment that harbours important regulatory functions such as contact to extracellular matrix and other cells, attachment and cell migration. Their induction and maintenance are completely dependent on an ongoing synthesis of HA by HAS, and their retraction occurs immediately after digestion with hyaluronidase, indicating that they are HA-dependent.[26] Nevertheless, using live cell microscopy, it has been demonstrated that these slender extensions in different orientations could be plasma membrane protrusions rather than just long extended HA chains arising from a flat cell surface. In other words, it is as if HA attached on plasma membrane is a prerequisite for membrane protrusions, and membrane protrusions are required to form a scaffold for the classical HA-coat.[17]

Consequently, we concluded that the broad protrusions extending from the cellular membrane of shar peis should serve as a support to the wide and concentrated HA extracellular distribution, while in controls, they were less expanded because of the lack of an active synthesis and release of HA in the extracellular compartment.

A clear and tangled network-like pattern of green fluorescence was also detected in the cytoplasm of fibroblast cells of both shar peis and controls (although in the latter group it was less intense), in accordance with previous studies.[22] The same fluorescence was shown to distribute as either diffuse network pattern or dense green particles at the edge of the cells especially in shar peis, and by time lapse microscopy on live cells it was demonstrated to disappear totally together with a retraction of cell membrane protrusions after 70 minutes from treatment of fibroblasts with hyaluronidase.

A complex interplay exists between HA synthesis, internalization and degradation, and a number of morphological observations suggest that there may be a relationship between intracellular HA and mitotic processes.[19-21] Indeed, HA has been associated with heterochromatin and nucleoli at which level signals mediating mitosis and increased motility are induced.[19,27-29] Moreover, HA has been also demonstrated to colocalize with a lysosomal marker, indicating that it may be destined in this compartment for degradation.[20]

In our study and as before mentioned, the fluorescein-labelled HA wasn’t restricted to nuclear zone

but it was demonstrated diffusely distributed in the cytoplasm and also at the periphery of cells as dense green vesicles that were hypothesized to correspond with focal points of active HA synthesis. Moreover, by TEM was possible to detect a high number of intracellular dense vesicles that were considered to correspond to lysosomes. Vesicles were mostly distributed under profuse lamellipodia and were clearly more abundant in shar peis than in controls. These findings were considered to be compatible with a cell with a highly active HA metabolism and suggested that a close relationship should occur between HA synthesis, uptake and degradation.

Scanning electron microscopy revealed that the surface of rounded fibroblasts was covered by individual fine strands periodically studded with bead-like corpuscles. Strands were more diffused on the surface of the rounded fibroblasts of shar peis than of the elongated fibroblasts of controls and appeared to extend from nodular and dense aggregates variously distributed on the edge of the cell.

According with previous studies,[19] these perpendicular strands were hypothesized to be individual HA chains, and the corpuscular aggregates that periodically decorate them, to be putative proteoglycans. Indeed, the numerous chondroitin sulfate chains of the proteoglycans have been considered to confer a high fixed negative charge density to the pericellular matrix and to have important effects on the permeability, viscosity and expansion of the coat volume.[18]

Consequently, we concluded that the binding and/or crosslinking of these corpuscles along these fine strands would dictate the viscosity of the extracellular environment. On the contrary, the nodule like structures from which the strands emanated were supposed to be one or more of the HA synthases or HA receptors such as reported in a recent study.[30] From a certain point of view, these findings were also in agreement with what supposed by confocal technique.

Taken together, the results of this work contributed to a better understanding of the mechanisms underlying the defect in the regulation of synthesis by HA dermal fibroblasts and to acquire new information on the impact that HA has on cellular behaviour in shar pei dogs.

## Acknowledgments

The authors wish to thank Dr. Thomas N. Wight from the Benaroya Research Institute at Virginia Mason, for his precious suggestions and evaluation of this article.

## FIGURES

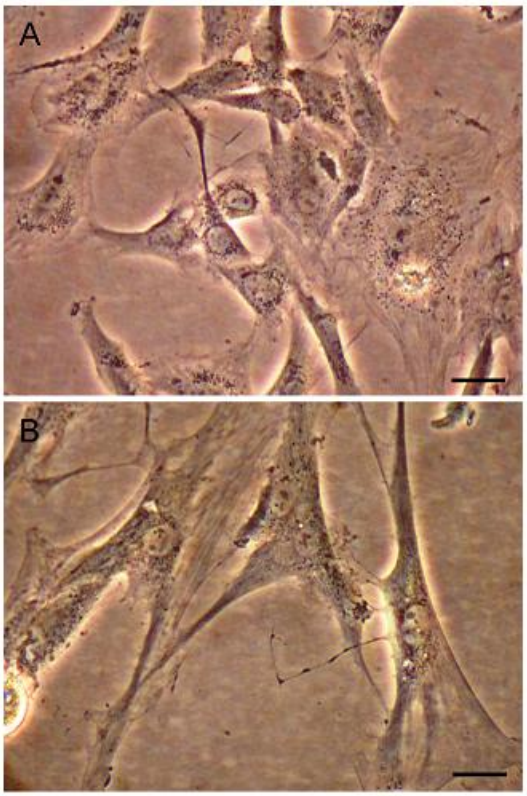


**Figure 1. Subconfluent fibroblasts cell cultures examined under Inverted Nikon microscope.** Fibroblasts from shar pei, show a rounded shape (A). Fibroblasts from control, show an elongated shape (B). Scale bar=40µm.

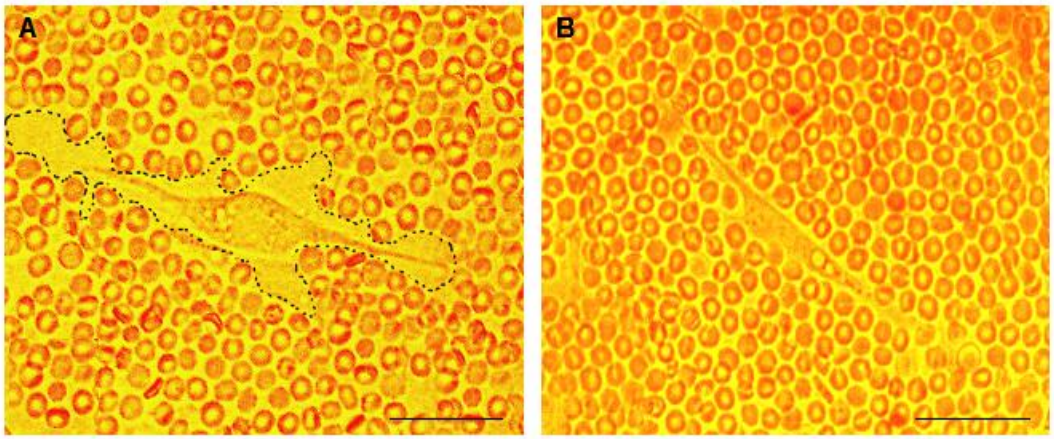


**Figure 2. Pericellular coat visualized by a particle-exclusion assay.** Fibroblast from shar pei, shows to exclude fixed erythrocytes from the surface as indicated by the dotted line (A). Fibroblast from control, shows red blood cells settled immediately adjacent to the cell surface (B). Scale bar=50µm.

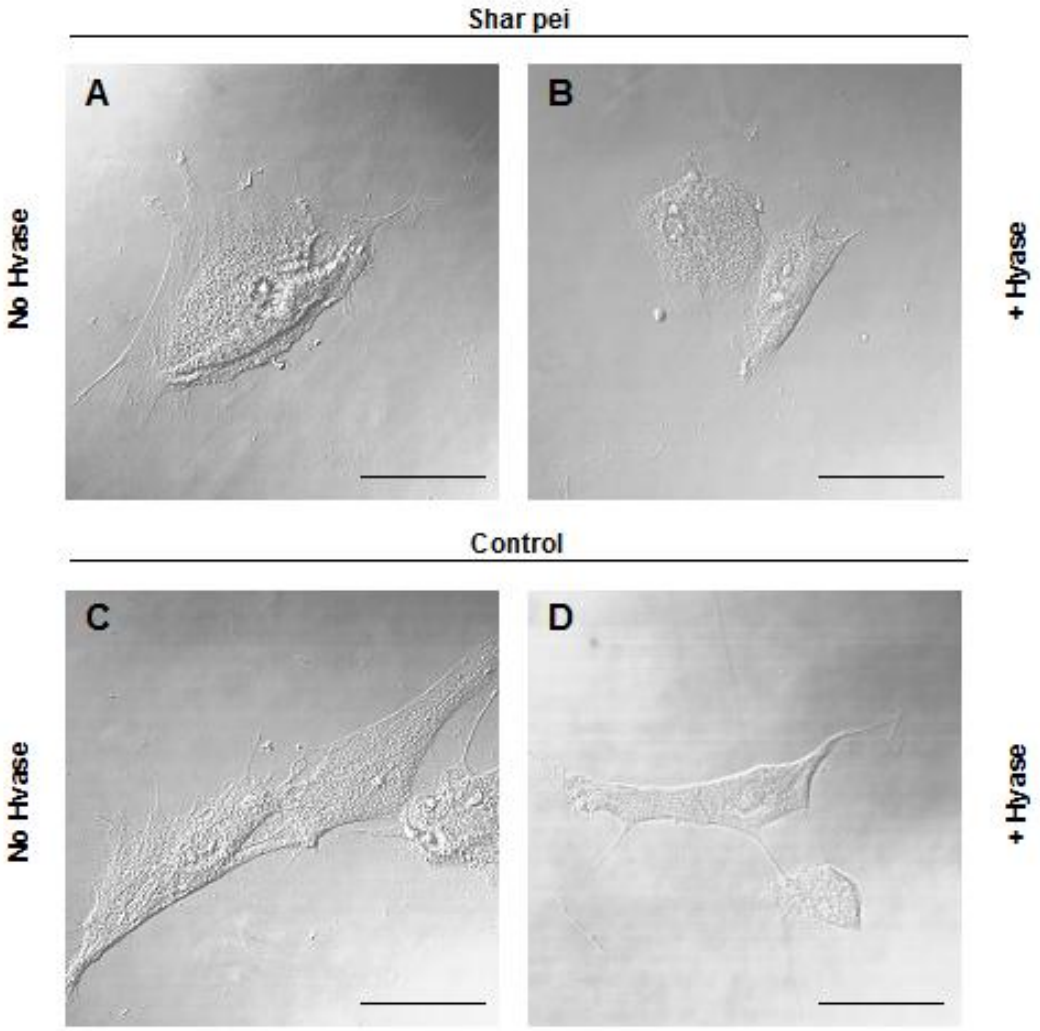


**Figure 3. Transmitted light images of fibroblasts from shar pei and control.** Fibroblast from shar pei, shows long and expanded protrusions extending from the edge of the cell (A). Fibroblasts from shar pei, with projections removed after digestion with hyaluronidase (B). Fibroblasts from control, show short protrusions projecting out from the cell surface (C). Fibroblasts from control, with projections removed after digestion with hyaluronidase (D). Scale bar=40µm

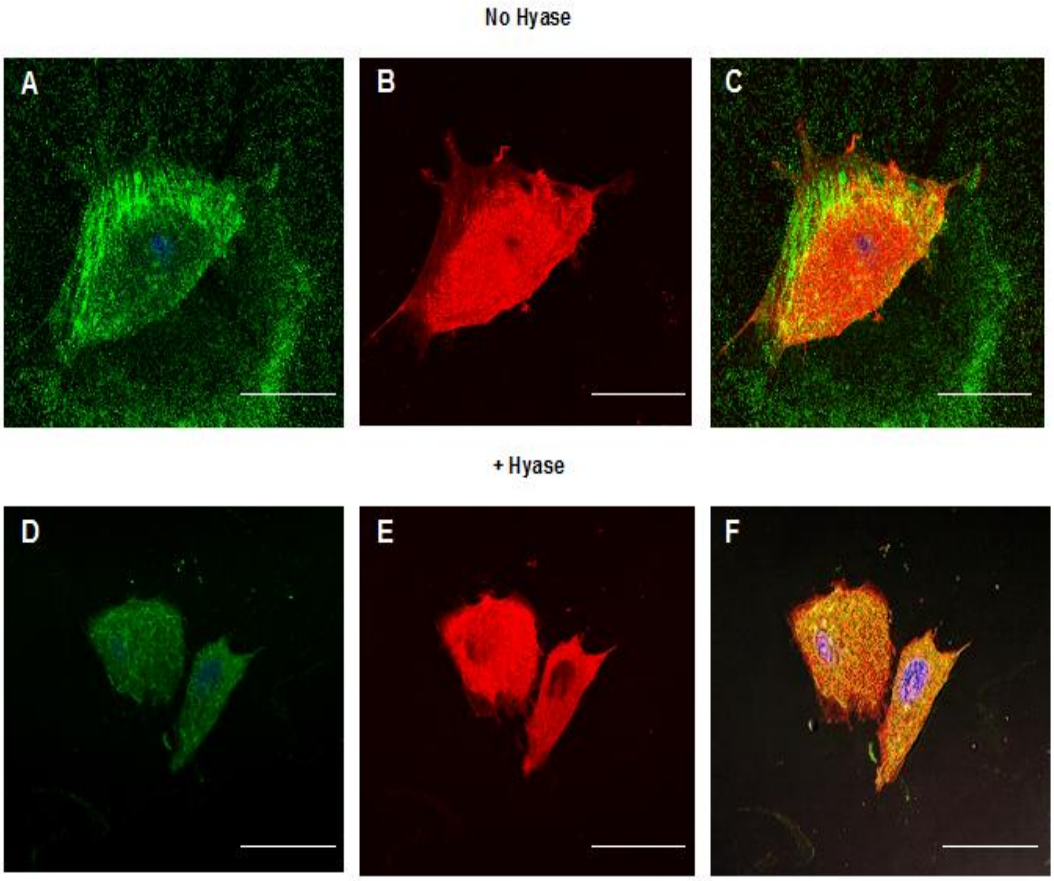


**Figure 4. Hyaluronic acid cellular localization in permeabilized fibroblasts from shar pei.** The fluorescein-labelled HA was detected as a green tangled flocculent network diffusely distributed around fibroblast and also intracellularly. Nuclei were counterstained with Hoechst 33342 (blue) (A). Fibroblast labelled with CellMask® cell membrane dye, showed broad expanded protrusions (B). Merging of both images (C). In fibroblasts labelled with bHABP, the extracellular green staining was digested after hyaluronidase treatment (D). Fibroblasts labelled with CellMask® cell membrane dye showed a retraction of protrusions after hyaluronidase digestion (E). Merging of both images (F). Scale bar=40µm.

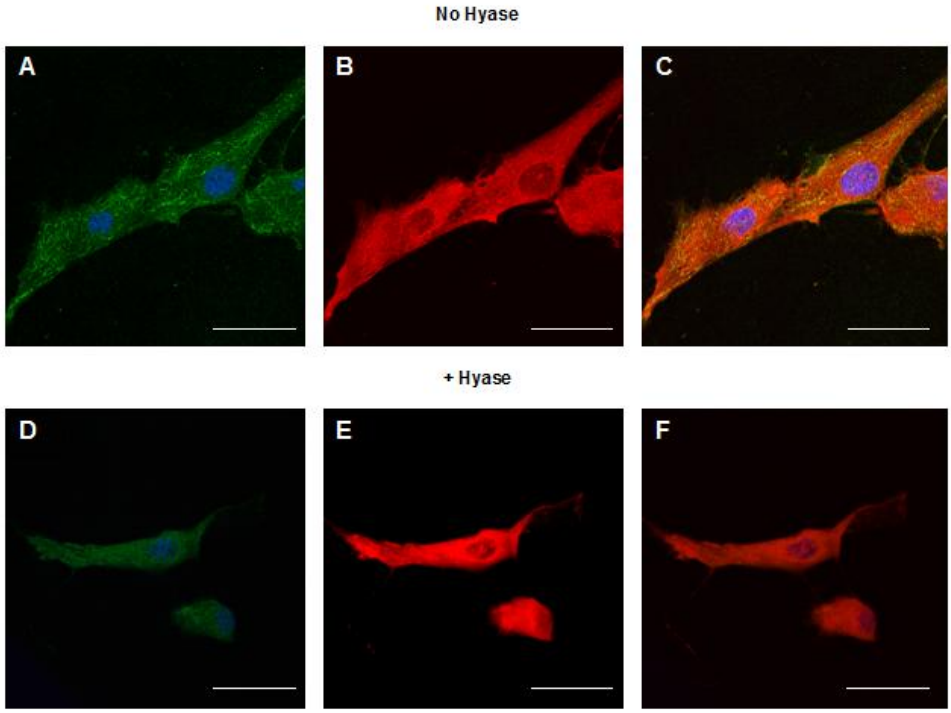


**Figure 5. Hyaluronic acid cellular localization in permeabilized fibroblasts from control.** The fluorescein-labelled HA was detected as a faint green extracellular staining. This staining was stronger intracellularly. Nuclei were counterstained with Hoechst 33342 (blue) (A). Fibroblasts labelled with CellMask® cell membrane dye showed short membrane protrusions (B). Merging of both images (C). Digestion of green staining after hyaluronidase treatment of fibroblasts labelled with bHABP (D). Fibroblasts labelled with CellMask® cell membrane dye showed a retraction of the short membrane protrusions (E). Merging of both images (F). Scale bar=40µm.

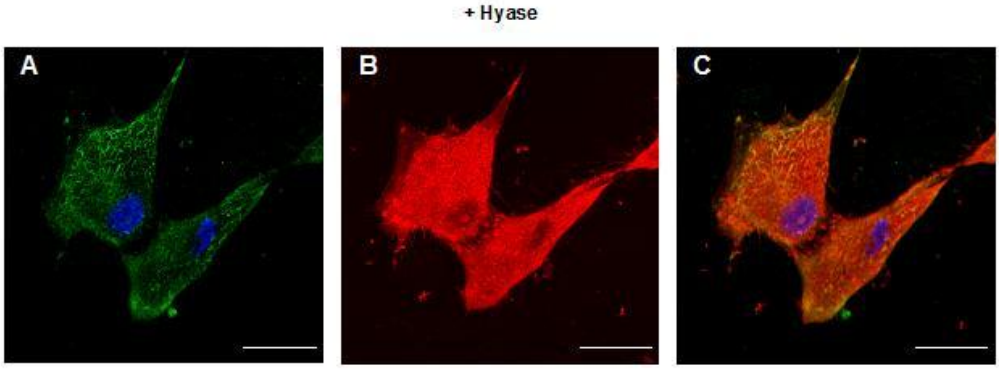


**Figure 6. Hyaluronic intracellular localization in hyaluronidase digested and permeabilized fibroblasts from shar pei.** The fluorescein-labelled HA was detected as a prominent cytoplasmic staining that appeared both in dense green particles and in diffuse green pattern throughout the cytoplasm of fibroblasts. Nuclei were counterstained with Hoechst 33342 (blue) (A). Fibroblasts were labelled with CellMask® cell membrane dye (B). Merging of both images (C). Scale bar=40µm.

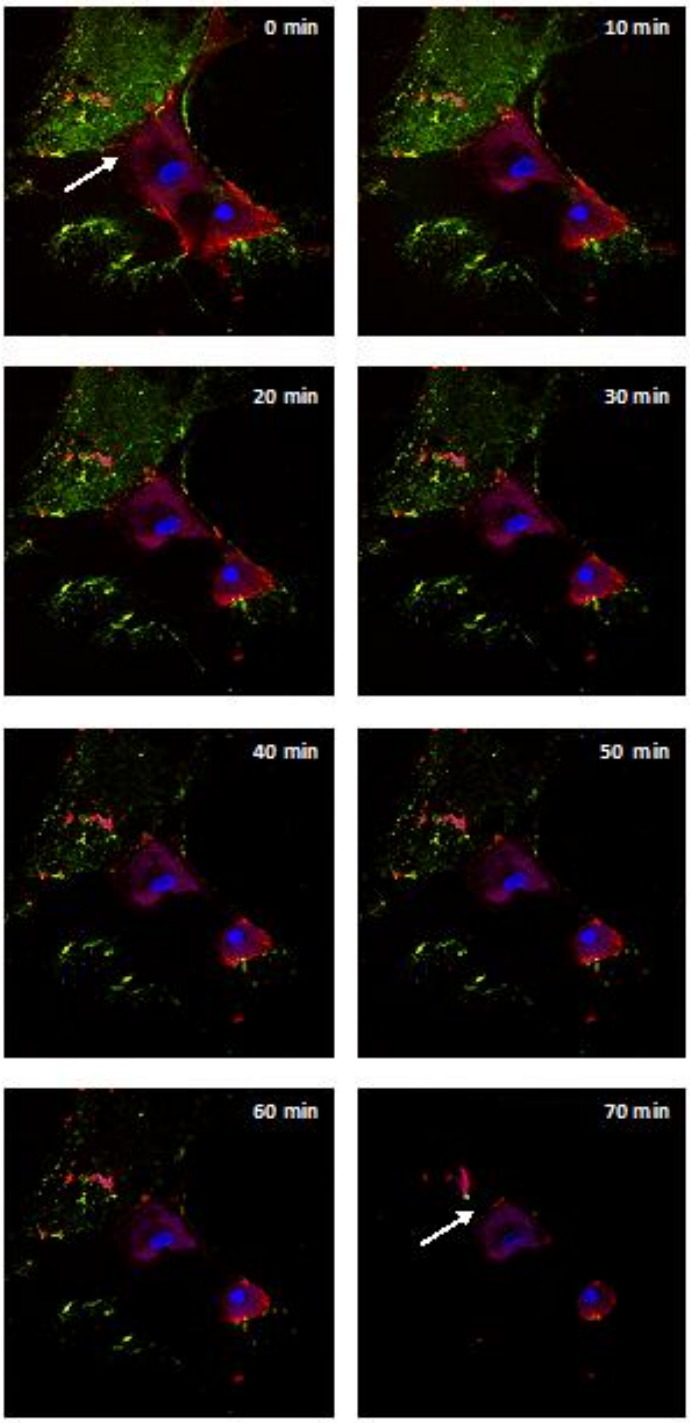


**Figure 7. Time lapse of living cells of shar pei treated with hyaluronidase.** The fluorescence-labelled HA was detected as a green staining, that completely disappeared after 70 minutes from digestion with hyaluronidase together with a retraction of membrane protrusions (arrow). Nuclei were counterstained with Hoechst 33342 (blue) and cell membrane with CellMask® (red). Scale bar=40µm

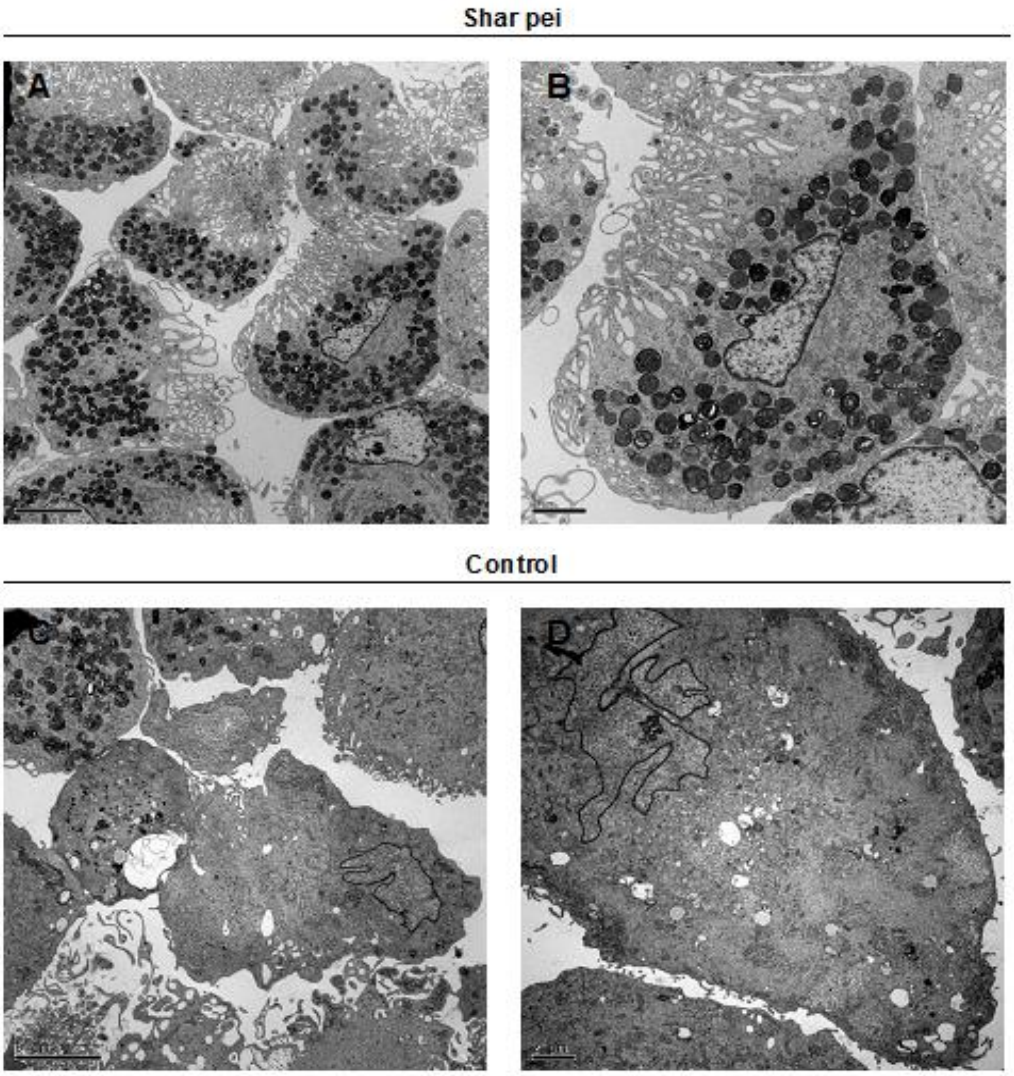


**Figure 8. Transmission electron microscopy of fibroblasts of shar pei and control.** Rounded fibroblasts from shar pei showed multiple convoluted lamellipodia-like protrusions polarized on a side of the cells. Intracellularly, presence of spherical dense particles corresponding to lysosomes (A). All these findings are better appreciated at higher magnification (B). In fibroblasts from control, protrusions appeared as few, thin, short structures diffusely distributed at cell surface. Intracellularly, scattered and less dense particles corresponding to lysosomes were detected (C). All these findings are better appreciated at higher magnification (D). Scale bar=5µm (A,C). Scale bar=2µm (B,D).

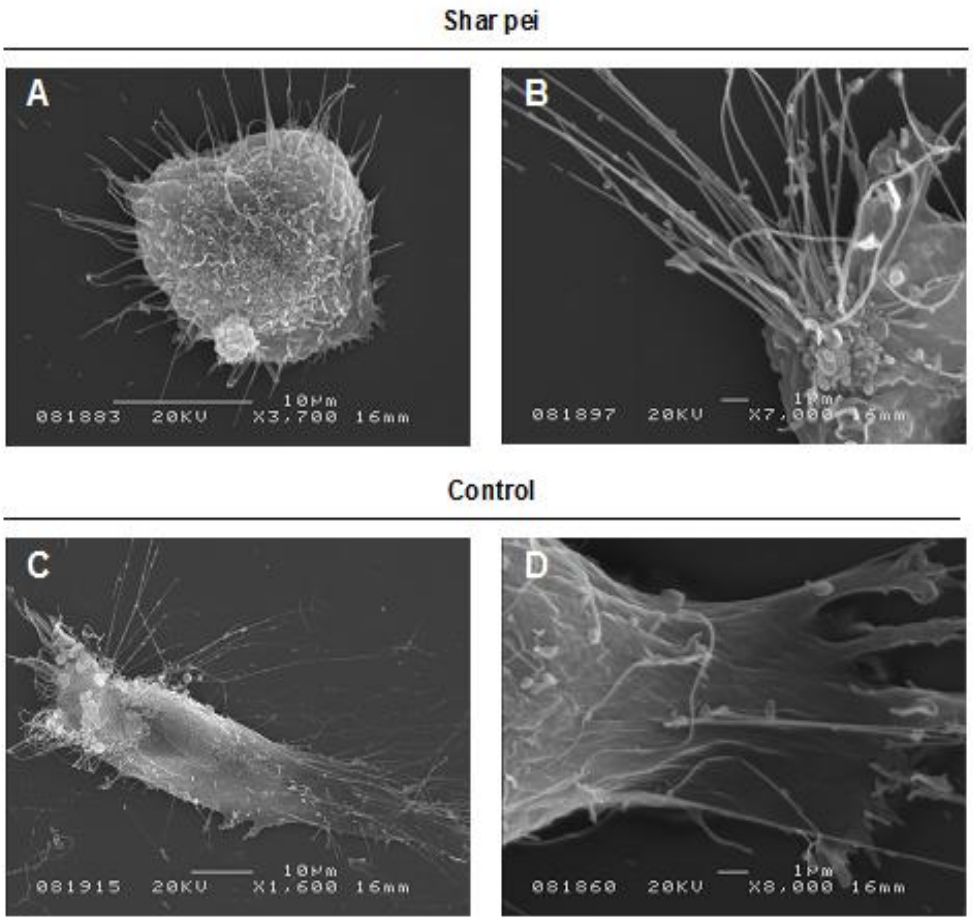


**Figure 9. Scanning electron microscopy of fibroblasts of shar pei and control.** In shar pei, slender microvillus-type protrusions were observed to emerge from the edge of cell membrane. Presence of a globular, dense corpuscle on the edge of the cell (A). Thin strands that emerged from condensed particles were decorated by rounded granules (B). Microvillous were less diffusely distributed on the surface of the elongated fibroblasts of control (C) and mostly emerging from the flanks of the cell as thin strands decorated by scattered granules (D). Scale bar=10 µm (A,C) and 1µm (B,D).

## References

1. von Bomhard D and Kraft W. Idiopathic mucinosis cutis in Chinese Shar pei dogs: epidemiology, clinical features, histopathologic findings and treatment. *Tierarztl Prax Ausg K Klientiere Heimtiere* 1998;26:189-96.

2. Zanna G, Fondevila D, Bardagi M, Docampo MJ, Bassols A, Ferrer L. Cutaneous mucinosis in shar-pei dogs is due to hyaluronic acid deposition and is associated with high levels of hyaluronic acid in serum. *Vet Dermatol* 2008;19:314-8.

3. Gross TL, Ihrke PJ, Walder EJ, Affolter VK. Disease of the dermis: cutaneous mucinosis. In: *Skin diseases of the dog and cat. Clinical and Histopathologic diagnosis*, Blackwell Publishing Ltd, 2nd Eds. Oxford, UK. 2005. p. 380-3.

4. Itano N and Kimata K. Molecular cloning of human hyaluronan synthase. *Biochem Biophys Res Commun* 1996;222:816-20.

5. Weigel PH, Hascall VC, Tammi M. Hyaluronan synthases. *J Biol Chem* 1997; 272:13997-4000.

6. Spicer AP and McDonald JA. Characterization and molecular evolution of a vertebrate hyaluronan synthase gene family. *J Biol Chem* 1998;273:1923-32.

7. Itano N and Kimata K. Mammalian hyaluronan synthases. *IUBMB Life* 2002;54:195-9.

8. Weigel PH and DeAngelis PL. Hyaluronan synthases: a decade-plus of novel glycosyltransferases. *J Biol Chem* 2007;282:36777-81.

9. Evanko SP, Johnson PY, Braun KR, Underhill CB, Dudhia J, Wight TN. Platelet-derived growth factor stimulates the formation of versican-hyaluronan aggregates and pericellular matrix expansion in arterial smooth muscle cells. *Arch Biochem Biophys* 2001;394:29-38.

10. Evanko SP, Tammi MI, Tammi RH, Wight TN. Hyaluronan-dependent pericellular matrix. *Adv Drug Deliv Rev* 2007;59:1351-65.

11. Li Y and Heldin P. Hyaluronan production increases the malignant properties of mesothelioma cells. *Br J Cancer* 2001;85:600-7.

12. Itano N, Sawai T, Atsumi F, Miyaishi O, Taniguchi S, Kannagi R, *et al*. Selective expression and functional characteristics of three mammalian hyaluronan synthases in oncogenic malignant transformation. *J Biol Chem* 2004; 279:18679-87.

13. Pienimaki JP, Rilla K, Fulop C, Sironen RK, Karvinen S, Pasonen S, *et al*. Epidermal growth factor activates hyaluronan synthase 2 in epidermal keratinocytes and increases pericellular and intracellular hyaluronan. *J Biol Chem* 2001;276:20428-35.

14.Kakizaki I, Kojima K, Takagaki K, Endo M, Kannagi R, Ito M, *et al*. A novel mechanism for the inhibition of hyaluronan biosynthesis by 4-methylumbelliferone. *J Biol Chem* 2004;279:33281-9.

15. Stuhlmeier KM and Pollaschek C. Glucocorticoids inhibit induced and non-induced mRNA accumulation of genes encoding hyaluronan synthases (HAS): hydrocortisone inhibits HAS1 activation by blocking the p38 mitogen-activated protein kinase signalling pathway. *Rheumatology* 2004;43:164-9.

16. Kultti A, Pasonen-Seppänen S, Jauhiainen M, Rilla KJ, Kärnä R, Pyöriä E, *et al*. 4-Methylumbelliferone inhibits hyaluronan synthesis by depletion of cellular UDP-glucuronic acid and downregulation of hyaluronan synthase 2 and 3. *Exp Cell Res* 2009;315:1914-23.

17. Rilla K, Tiihonen, Kultti A, Tammi M, Tammi R. Pericellular hyaluronan coat visualized in live cells with a fluorescent probe is scaffolded by plasma membrane protrusions. *J Histochem Cytohistochem* 2008;56:901-10.

18. Evanko S, Angello J, Wight T. Formation of hyaluronan and versican rich pericellular matrix is required for proliferation and migration of vascular smooth muscle cells. *Arterioscler Thromb and Vasc Biol* 1999;19:1004-13.

19. Evanko SP and Wight TN. Intracellular localization of hyaluronan in proliferating cells. *J Histochem Cytochem* 1999;47:1331-41.

20. Evanko SP, Parks WP, Wight TN. Intracellular hyaluronan in arterial smooth muscle cells: association with microtubules, RHAMM, and the mitotic spindle. *J Histochem Cytochem* 2004;52:1525-35.

21. Hascall VC, Majors AK, De La Motte CA, Evanko SP, Wang A, Drazba JA, *et al*. Intracellular hyaluronan: a new frontier for inflammation? *Biochim Biophys Acta* 2004;1673:3-12.

22. Zanna G, Docampo MJ, Fondevila D, Bardagi M, Bassols A, Ferrer L. Hereditary cutaneous systemic mucinosis in shar pei dogs is associated with increased hyaluronan synthase-2 mRNA transcription by cultured dermal fibroblasts. *Vet Dermatol* 2009;20:377-82.

23. Serra M, Rabanal RM, Miquel L, Domenzain C, Bassols A. Differential expression of CD44 in canine melanocytic tumours. *J Comp Pathol* 2004;130:171-80.

24. Brecht M, Mayer U, Schlosser E, Prehm P. Increased hyaluronate synthesis is required for fibroblast detachment and mitosis. *Biochem J* 1986;239:455-60.

25. Hunzinker EB and Schenk RK. Cartilage ultrastructure after high pressure freezing, freeze substitution, and low temperature embedding. Intercellular matrix ultrastructure-preservation of proteoglycans in their native state. *J Cell Biol* 1984; 98:277-82.

26. Kultti A, Rilla K, Tiihonen R, Spicer AP, Tammi RH, Tammi MI. Hyaluronan synthesis induces microvillus-like cell surface protrusions. *J Biol Chem* 2006; 281:15821-8.

27. Londono I and Bendayan M. High-resolution cytochemistry of neuraminic acid and hexuronic acid-containing macromolecules applying the enzyme-gold approach. *J Histochem Cytochem* 1988;36:1005-14.

28. Ripellino JA, Margolis RU, Margolis RK. Immunoelectron microscopic localization of hyaluronic acid-binding region and link protein epitome in brain. *J Cell Biol* 1989;108:1899-907.

29. Kan FW. High resolution localization of hyaluronic acid in the golden hamster oocyte-cumulus complex by use of a hyaluronidase-gold complex. *Anat Rec* 1990; 228:370-82.

30. Evanko SP, Potter-Perigo S, Johnson PY, Wight TN. Organization of hyaluronan and versican in the extracellular matrix of human fibroblasts treated with the viral mimetic, poly I:C. *J Histochem Cytochem* 2009;57:1041-60.